RSC Sustainability

ROYAL SOCIETY OF CHEMISTRY

PAPER

View Article Online
View Journal | View Issue

Cite this: *RSC Sustainability*, 2023, **1**, 2341

Direct re-lithiation strategy for spent lithium iron phosphate battery in Li-based eutectic using organic reducing agents†

Tanongsak Yingnakorn,[a] Jennifer Hartley,[a] Jason S. Terreblanche,[a] Chunhong Lei,[a] Wesley M. Dose[ab] and Andrew P. Abbott *[a]

Received 11th July 2023
Accepted 1st November 2023

DOI: 10.1039/d3su00237c

rsc.li/rscsus

One of the most commonly used battery cathode types is lithium iron phosphate ($LiFePO_4$) but this is rarely recycled due to its comparatively low value compared with the cost of processing. It is, however, essential to ensure resource reuse, particularly given the projected size of the lithium-ion battery (LIB) market. A simple, green, inexpensive, closed-loop process is proposed for recycling $LiFePO_4$ cathodes, *via* delamination of the cathode active material from the aluminium current collector by simple immersion in water. Two regeneration routes are compared to demonstrate how recovered $Li_{1-x}FePO_4$ can be regenerated: (1) direct re-lithiation of the spent cathode material under ambient temperature and pressure using a eutectic system made from lithium acetate and ethylene glycol with hydroquinone as a reducing agent, and (2) oxidative leaching of lithium ions in water, with iron(III) chloride as an oxidising agent, followed by regeneration back to the $LiFePO_4$ olivine structure using same re-lithiation method. The use of this non-aqueous lithium-based eutectic system in combination with a reducing agent decreases the temperature and number of steps required for the regeneration of $LiFePO_4$ and restores the electrochemical performance of the spent material.

Sustainability spotlight

Direct re-lithiation strategy for spent lithium iron phosphate battery in Li-based eutectic using organic reducing agents. This paper addresses the UN's Sustainability Development Goal #7 of creating affordable and clean energy. Central to this goal is the development of electric vehicles and the ability to store renewable energy at home. Lithium iron phosphate (LFP) is key to this drive as it is used in low-cost lithium-ion batteries which is made largely of earth abundant elements. The issue with creating circularity with LFP batteries is that the cost of regenerating them is high due to complex, multi-step, high temperature processes. In this paper we demonstrate the first low temperature, single-step regeneration of lithium iron phosphate cathode material using simple, common starting materials. There is also the potential to create this as a circular catalytic process.

Introduction

Lithium-ion batteries (LIBs) with a lithium iron phosphate ($LiFePO_4$, LFP) positive electrode are widely used for a variety of applications, from small portable electronic devices to electric vehicles (EVs). The LFP-type LIB market is growing rapidly due to advantages such as cost, safety, and use of non-critical and earth abundant Fe, rather than Ni and Co.[1,2] It is forecast that LFP will claim an increasing proportion of the LIB market share in applications such as stationary storage (coupled to renewable energy generation such as wind and solar) and EVs.

However, the large number of batteries in EVs and stationary energy storage applications coming to their end-of-life is generating increasing amounts of spent battery materials, presenting a challenge to recover the active materials in a profitable process.[3–5] Recycling of spent batteries is crucial to establish a circular economy for high-value resources and to protect the environment.[6] Currently, the most common recycling technology for LFP cathodes is hydrometallurgy,[7] which involves a series of leaching and precipitation steps to recover high-purity metals or compounds,[8,9] followed by mixing and calcination of recovered products at high temperatures to regenerate $LiFePO_4$.[10,11] However, traditional hydrometallurgical recycling routes are practically challenging due to complex processing, high amounts of reagents and energy consumed, and the inevitable wastewater treatment costs.

Alternatively, direct regeneration of degraded cathode materials, a non-destructive technique to reintroduce lithium after repeated cycles, is a more efficient recycling approach.[12,13]

[a]*School of Chemistry, University of Leicester, Leicester, LE1 7RH, UK. E-mail: apa1@le.ac.uk*

[b]*School of Chemistry, University of New South Wales, Sydney, NSW 2052, Australia*

† Electronic supplementary information (ESI) available. See DOI: https://doi.org/10.1039/d3su00237c

All the life-cycle assessment criteria could be significantly improved if materials are not reduced to their elemental or precursor salt forms before regeneration. One of the largest contributors to the cost of recycling cathode materials is the high temperature regeneration with Li sources (such as Li_2CO_3, LiOH, and Li_3PO_4) usually about 550 to 800 °C for 7 to 48 hours under argon or nitrogen atmosphere.[14,15] See Table S1† for more examples of LFP synthesis. Direct regeneration has previously been shown for $LiCoO_2$ using molten salt systems, such as a eutectic mixture of LiCl and CH_4N_2O containing a small amount of CoO for the selective replenishment of lithium and cobalt at 120 °C,[16] or the use of a molten lithium nitrate system at 300 °C to regenerate $LiFePO_4$, with sucrose as a reducing agent.[17] While these direct regeneration processes have provided a lower temperature route to regeneration of spent cathode materials, there is still room for improvement due to the fact that temperatures of >100 °C are still being employed, and that there are potential safety concerns due to the highly oxidising behaviour of lithium nitrate.

A low temperature alternative involves the use of deep eutectic solvents (DESs), which are composed of a bulky organic cation (commonly quaternary ammonium salts) and a hydrogen bond donor (HBD). These have the advantage of minimising water use, and have often been described as having the ability to be "tailored" to achieve specific physical and chemical properties.[18] They are easy to prepare under ambient conditions, and have previously been used for the extraction and recovery of desired metals from various materials on large scales, including spent EV batteries.[19–21] The majority of these studies have focussed on lithium nickel manganese cobalt oxides ($LiNi_xMn_yCo_{1-x-y}O_2$, NMC) and lithium cobalt oxide ($LiCoO_2$, LCO) chemistries. For example, the recovery process of LCO by leaching of Li and Co in the choline chloride: urea DES at 180 °C for 12 h obtained a 95% leaching efficiency, where Co was recovered as cubic cobalt oxide spinel (Co_3O_4) after a precipitation–calcination process using $H_2C_2O_4$ and NaOH precipitants.[22] Similarly, the mixture of oxalic acid dihydrate and choline chloride was used as a DES for dissolving Li, Mn, and Co from NMC and the Mn and Co were thereafter precipitated by the simple addition of water to form mixed metal oxalates.[23] Metal recovery from battery leachates has also been carried out *via* solvent extraction methods, from both DES and aqueous systems. For example, Zante *et al.* show that hydrophobic eutectic systems made from lidocaine with decanoic acid or lauric acid can be used to leach battery materials, with *N*,*N*,*N*′,*N*′-tetra(*n*-octyl) diglycolamide being used to extract the Mn.[24] A series of different solvent extraction steps have been used by Schiavi *et al.* to selectively recover Mn and Co from a DES formed from choline chloride and ethylene glycol, resulting in the production of cobalt oxalate. The DES was shown to be reusable, despite the high temperatures (90 to 160 °C) used during both leaching and extraction.[25] Likewise, a choline chloride–citric acid DES diluted with water was proposed as a lixiviant for LCO at 40 °C for 1 h, which uses metallic aluminium and copper as reducing agents. The copper and 98% leached cobalt could be recovered from the pregnant leach solution by non-aqueous solvent extraction by LIX 984 and Aliquat 336, respectively.[26] Bis(2-ethylhexyl) phosphoric acid has been used in battery recycling processes for the extraction of Cu, Co, Mn, and Ni from acidic aqueous solutions,[27,28] whereas tri-*n*-butyl phosphate-sulfonated kerosene has been used to successfully extract Li and Fe from spent LFP, where $FeCl_3$ was used as a leaching agent.[29]

The remaining challenge of recycling LFP-type batteries is regeneration in a sustainable, low-cost, and low-energy process. It has previously been estimated that the cost of recycling LIB cathodes must be in the range $2–6 per kg,[30] and the regeneration costs of $LiFePO_4$ must be towards the low end of that range due to the lower intrinsic material value when compared to nickel or cobalt-containing battery chemistries. Therefore, it is essential to use simple, fast, and selective processes with minimal chemical and energy inputs. The present research addresses this gap by demonstrating the use of a eutectic mixture formed from lithium acetate, as a lithium source, and ethylene glycol, as an HBD, in combination with organic reducing agents, to regenerate spent $Li_{1-x}FePO_4$ cathode materials without destroying the crystal structure at room temperature. The effect of direct reductive re-lithiation is compared with a two-step oxidative leaching (lithium extraction)-reductive regeneration process.

Experimental

Materials

The chemicals used were ethylene glycol (EG, Sigma Aldrich, >98.0%), iron(III) chloride ($FeCl_3$, Merck, >98.0%), lithium acetate dihydrate ($LiOAc{\cdot}2H_2O$, Thermo scientific, >98.0%), hydroquinone (Acros organics, 99.5%), L-ascorbic acid (Sigma Aldrich, 99%), oxalic acid ($C_2H_2O_4$, Aldrich, 98%, β-D-glucose (Sigma, ≥99.5%), catechol (Lancaster, >98.0%), commercial lithium iron phosphate ($LiFePO_4$, Hydro-Québec, Carbon coated), carboxymethylcellulose/styrene butadiene rubber (CMC/SBR, $M_w \sim 250\,000$ Sigma Aldrich, MTI Corp, EQ-Lib-SBR model), polyvinylidene fluoride (PVDF, Alfa Aesar), conductive carbon black (Timcal Super C45, Cambridge energy solutions), *n*-methyl-2-pyrrolidone (NMP, Acros organics, 99.5%), dimethyl carbonate (DMC, Sigma-Aldrich, 99%) and a spent lithium iron phosphate battery (CALB, 130 Ah). The spent electrode materials were washed with DMC to remove the electrolyte and dried prior to them being received.

Solvent preparation

The lithium acetate eutectic intended for use as a lithium source for regeneration of $LiFePO_4$ was prepared by mixing lithium acetate dihydrate and ethylene glycol in a molar ratio of 1 : 3 at a temperature of 60 °C, until a homogenous liquid had formed. This solvent will be referred to as $LiOAc{\cdot}2H_2O$:3EG, and was stored in a sealed glass vessel at room temperature until required. The organic reducing agents (L-ascorbic acid, catechol, hydroquinone, oxalic acid, or β-D-glucose) were dissolved in the $LiOAc{\cdot}2H_2O$:3EG eutectic at concentrations of 0.55 mol per mol of $FePO_4$ (mol ratio of $FePO_4$, $LiOAc{\cdot}2H_2O$:3EG, and the reducing agent is 1 : 1.1 : 0.55) immediately

before use to minimise any potential side reactions. This was equivalent to *ca.* 0.4 g of hydroquinone per 1 g of spent $Li_{1-x}FePO_4$ in 2.1 g of the $LiOAc \cdot 2H_2O$:3EG solution.

The solution used for oxidation of $LiFePO_4$ was prepared by dissolving 1.0 mol dm^{-3} $FeCl_3$ in water with stirring and heating at 60 °C until all solids had dissolved. The mixture was also stored in a sealed glass vessel at room temperature until required, in order to minimise variations in moisture content.

The solutions for voltammetric profiling were prepared by dissolving 0.02 dm^{-3} of L-ascorbic acid, catechol, β-D-glucose, hydroquinone, or oxalic acid in the relevant solvent at 50 °C.

Instrumentation

To study potential windows of reducing agents in $LiOAc \cdot 2H_2O$:3EG involved with the re-lithiation step, 5 mm diameter glassy carbon disk, platinum flag, and aqueous 3.0 mol dm^{-3} KCl silver/silver chloride electrodes were used as the working, counter, and reference electrodes, respectively. The glassy carbon disk electrode was cleaned by polishing in a slurry of 0.02 μm alumina paste, before being rinsed with deionised water and dried in air. A potential step of 2 mV and a scan rate of 20 mV s^{-1} was selected for all experiments.

SEM and EDX were used to determine the thickness of the cathode cross sections, and analyse the solid powder morphology and elemental composition with an FEI Quanta 650 FEG in backscattered electron mode at 20 kV and 5 nm spot size with Aztec controlling software. X-ray diffraction patterns of powders in this work were measured using a Phillips PW 1730 X-ray generator, with a PW 1050/25 detector and a PW 1716 diffractometer operating at 40 kV and 30 mV and controlled by DIFFRAC.COMMANDER software. All samples were prepared in polymethyl methacrylate (PMMA) specimen holders of 8.5 mm in height, sample reception 25 mm in diameter, and were measured at a scan range between 10° to 90° 2θ and a step size of 0.02°. The obtained X-ray diffraction peaks were analysed and matched with the database included in the DIFFRAC.EVA software.

Thermogravimetric analysis differential scanning calorimetry (TGA-DSC) was carried out using a Mettler Toledo TGA/DSC1 machine with a resolution of ±1 μg and a maximum temperature of 1100 °C, controlled by STARe software (version 12.10). The balance used to weigh the samples was a Mettler Toledo Semi-Micro Balance (MS105DU), with a resolution of 0.1 mg. The samples (30–40 mg) were placed in 100 μL aluminium crucibles with no lid. The temperature that operated in the program was from 25 to 550 °C with 5 °C min^{-1} of a heating rate and 20 mL min^{-1} of a nitrogen flow. Reference materials were prepared for TGA-DSC by forming a slurry of the commercial $LiFePO_4$ with carbon black and different known binders at a weight ratio of 90 : 5 : 5, using a method adapted from Scott *et al.*[31] The PVDF sample was prepared using NMP as a solvent, whereas the CMC-SBR (1 : 1 weight ratio) sample was prepared using water. The homogeneous slurry was coated onto aluminium foil. Then, the coated cathode was dried on a hot plate at 100 °C for about 1 h in the air. The cathodes were cut into small pieces (*ca.* 3 mm by 3 mm) and put into 100 μL aluminium crucibles with no lids for analysis.

The elemental composition of the spent $Li_{1-x}FePO_4$ powder was analysed using a Thermo Scientific iCAP Qc ICP-MS. Raw active material was digested in aqua regia and diluted by 200 000 times using 2 vol% nitric acid (Trace metal grade, Fisher Scientific), equivalent to 0.45 mol dm^{-3}, in order to be within the calibration range of 10 to 2000 ppb. The calibration curve was prepared using Spex CertiPrep, Multi-element Solution 2A, containing Ag, Al, As, Ba, Be, Ca, Cd, Co, Cr, Cs, Cu, Fe, Ga, K, Li, Mg, Mn, Na, Ni, Pb, Rb, Se, Sr, Tl, U, V, and Zn, all at 10 μg mL^{-1} (10 ppm) in 5% HNO_3, and Spex CertiPrep, Multi-element Solution 4, containing B, Ge, Mo, Nb, P, Re, Si, S, Ta, Ti, W, and Zr, all at 10 μg mL^{-1} (10 ppm) in trace HF and HNO_3. Also, the internal standards (spikes) were applied to all samples, using 50 μL of 1 ppm of rhodium (Merck, 10 mg kg^{-1} Rh in HNO_3) and lanthanum (Fisher Scientific, 1000 μg mL^{-1} in 2–5% HNO_3, Spex CertiPrep) for every 5 mL of samples to ensure measurement accuracy. Between the calibration curve and each group of 15 samples, three wash solutions of the 2 vol% nitric acid were recorded, also containing the internal standards. The 56Fe and 57Fe measurements are made in KED mode, whereas 6Li, 7Li, and 31P are made in STD mode. The calibration curves can be found in the ESI (Fig. S9v).†

$LiFePO_4$ regeneration procedure

Initially, the spent $Li_{1-x}FePO_4$ cathodes were delaminated in deionised water for 30 minutes at room temperature to separate cathode layers from aluminium foil, followed by a drying step at 80 °C for 2 h. This brittle and flaky material was ball milled at 200 rpm for 20 min to obtain a fine powder, which was used as the raw material for the leaching process and direct re-lithiation. The chemical composition of the active cathode material after delamination and grinding, as determined *via* ICP, is *ca.* 3.0–4.0 wt% of lithium, 14–18 wt% phosphorus, and 25–30 wt% iron (atomic ratio of Li : Fe : P is 0.91 : 1.00 : 0.99, which will be referred to as $Li_{0.91}FePO_4$).

Two regeneration methods were investigated: (1) direct re-lithiation without a preceding oxidative step, and (2) oxidative leaching of the spent $Li_{0.91}FePO_4$, followed by a re-lithiation step. In the first procedure, spent $Li_{0.91}FePO_4$ was directly re-lithiatiated by using 5 different organic reducing agents (L-ascorbic acid, catechol, hydroquinone, oxalic acid, or β-D-glucose), with $LiOAc \cdot 2H_2O$:3EG as both the solvent and the lithium source. The delaminated $Li_{0.91}FePO_4$ (1 g) was suspended in the solution, containing a 10% molar excess of lithium and reducing agent, and stirred for 1 to 3 h at 25 °C. Finally, the regenerated $LiFePO_4$ was separated by filtering, washed with water, and dried in an oven at 60 °C for 1 h.

In the second procedure, $Li_{0.91}FePO_4$ powder (0.5 to 2.5 g) was leached for 5 minutes to 3 h in water (10 mL) containing 0.1 to 1.0 mol dm^{-3} of $FeCl_3$, at temperatures of 25 to 50 °C. This was carried out in order to leach all remaining lithium from the $Li_{0.91}FePO_4$ powder. All investigated systems were heated and stirred at 500 rpm on a hot plate with a thermocouple until the reaction was complete. Afterwards, the solutions were filtered, washed with water, and the remaining solids dried in an oven at 60 °C for 1 h to obtain the iron phosphate ($FePO_4$) powder. The

$FePO_4$ powder obtained after oxidative leaching was re-lithiated to form $LiFePO_4$, using the same procedure as for direct re-lithiation.

Electrochemical testing

The spent $Li_{0.91}FePO_4$ and re-lithiated powder were prepared by heating to 450 °C for 1 h in an argon atmosphere to pyrolyse the remaining polymer binder. Electrodes were prepared by forming a slurry of the active cathode materials, conductive carbon, and PVDF at a weight ratio of 90 : 5 : 5 in NMP. The homogeneous slurry was coated on aluminium foil and dried on a hot plate at 80 °C for about 2 h in the air. The prepared cathode sheet had an active loading of 8 mg cm^{-2}. The CR2032 coin cell parts, separators, and electrodes were dried under vacuum at 120 °C for 24 h and assembled in a glove box under a high-purity argon atmosphere ($H_2O \leq$ 1 ppm, $O_2 \leq 0.1$ ppm). The cells were comprised of the 14 mm $LiFePO_4$ cathodes, 15.7 mm lithium metal disc (PI-KEM) counter/reference electrodes and 16 mm glass fibre disc (Whattman) separators. 40 μL of LP57 (1 M $LiPF_6$ in ethylene carbonate (EC) : ethyl methyl carbonate (EMC) 3 : 7 vol%, Solvionic) was used as the electrolyte. The electrochemical properties of the $LiFePO_4$ materials were tested by a BSC-805 battery cycler (BT-Lab software, BioLogic). Charge/discharge was carried out at different current rates in a 2.8–3.8 V (*vs.* Li^+/Li) voltage window to study the electrochemical cycling performance. Cyclic voltammetry was carried out between 2.0 and 4.5 V (*vs.* Li^+/Li) at a scanning rate of 0.2 mV s^{-1}.

The initial carbon amount in the active material samples was measured by leaching the $LiFePO_4$ compound with aqua regia at 60 °C for 24 h from the powder, then filtering to weigh the remaining carbon content, with the chemical composition of the remaining solid confirmed by EDX.

Results and discussion

The end-of-life LIB pouch cell (130 Ah) used in this study (Fig. 1a) contains double-sided electrodes of LFP on aluminium foil as the positive electrode, referred to as the cathode, and graphite on copper foil as the negative electrode, or anode. The cathode coating is 80–90 μm thick (Fig. S1†) with EDX confirming the expected Fe : P : O elemental ratio, as shown in Table S2.† Soaking the cathode in water facilitates complete separation of the LFP coating from the current collector foil, as shown in Fig. 1b. Thermal analysis of the electrode facilitates identification of the binder as water soluble CMC-SBR (Fig. S2,† which likely facilitates the rapid delamination. Analysis of the resulting powder using ICP-MS and XRD (Fig. S3†) show the expected loss of lithium from the structure as a result of capacity fade in the cell, with the stoichiometry determined by ICP-MS ($Li_{0.91}FePO_4$, oxygen ratio is assumed to not change) in close agreement with the phase fractions determined from Rietveld refinement of the diffraction pattern (88(2) vol% $LiFePO_4$ and 12(1) vol% $FePO_4$). The low lithium stoichiometry highlights the need for simple and cost-effective methods to re-lithiate LFP extracted from end-of-life batteries.

Two approaches are investigated in this study (Fig. 1c). The first uses an organic reducing agent in a lithium acetate ethylene glycol eutectic ($LiOAc \cdot 2H_2O$:3EG) to directly re-lithiate the spent LFP material. In the second approach the material is first oxidised to $FePO_4$, using a 0.75 M iron(III) chloride ($FeCl_3$) solution as an oxidising agent, followed by re-lithiation as per the first approach. This two-step process was examined since processes that isolate the high-value lithium are industrially relevant.

Five organic reducing agents (L-ascorbic acid, catechol, hydroquinone, β-D-glucose, and oxalic acid) were screened for suitability to reduce $FePO_4$ in the $LiOAc \cdot 2H_2O$:3EG eutectic using cyclic voltammetry and XRD ($FePO_4$ was used as a model compound to highlight the wide applicability of the method, even for materials from cells with very low state-of-health (SOH)). These reducing agents were selected because they have been used in several industries, are bulk commodity chemicals, and are registered with registration, evaluation, authorisation and restriction of chemicals (REACH). Complex quinones have been previously shown to lithiate spent NMC successfully in organic media in the presence of lithium metal.[32] Cyclic voltammograms of the reducing agents in the eutectic (Fig. S4a†) show that only L-ascorbic acid, catechol, and hydroquinone present significant redox-active behaviour within the stability window of the eutectic. However, only hydroquinone displays reversibility, which is critical for a redox-recyclable reducing agent (Fig. 2a). The benefit of a recyclable reducing agent is that it imparts a measure of environmental sustainability into the process, as the amount of process waste generated is minimised, as are the raw chemical inputs. Powder XRD confirms that hydroquinone is an effective reducing agent for $FePO_4$ in the lithium-containing eutectic (Fig. 2b), with full conversion of $FePO_4$ to $LiFePO_4$, as per the reaction in Fig. 2c – the XRD patterns showing the effectiveness of the other reducing agents are provided in Fig. S5.† Moreover, quinones (110.11 g mol^{-1}) have an additional advantage over ascorbic acid (176.12 g mol^{-1}) as the latter needs to be used in higher amounts because of its higher molecular weight. Hence, only hydroquinone was carried forward into the following investigations where the two approaches were applied to regenerate the $Li_{0.91}FePO_4$ powder extracted from end-of-life cells.

Materials regenerated by direct re-lithiation (0.4 g of hydroquinone per 1 g of spent $Li_{0.91}FePO_4$ in 2.1 g of $LiOAc \cdot 2H_2O$:3EG at 25 °C) were characterised by XRD, SEM, and ICP-MS to understand the efficacy of this approach. Powder XRD patterns of the material after treatment for 0.5, 1, and 2 h are shown in Fig. 3a. The patterns show partial re-lithiation after 0.5 h – reflections characteristic of $FePO_4$ and $LiFePO_4$ are present – but after 1 h full conversion to $LiFePO_4$ has taken place, with no further changes in the structure following 2 h of treatment. Sharp reflections in the diffraction patterns indicate that the material exhibits good crystallinity, as required for effective battery performance. Fig. 3b and c show SEM micrographs of the cathode particles before and after direct re-lithiation. The particle shape and size remain unchanged. Elemental analysis of the eutectic solution after re-lithiation by ICP-MS reveals <50 ppm of Fe and P, demonstrating negligible leaching and

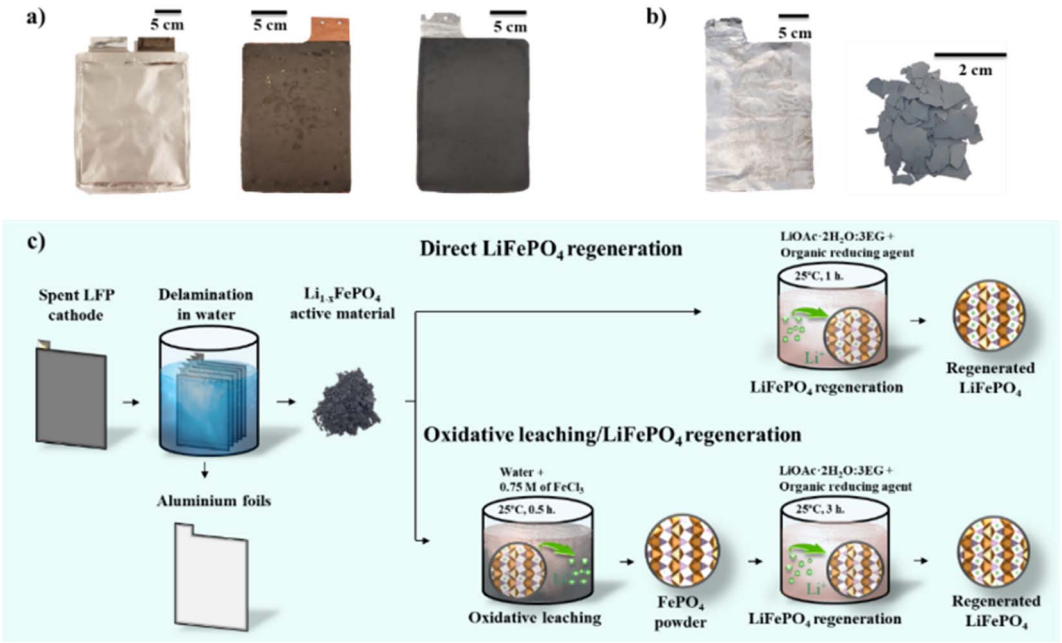

Fig. 1 (a) Dismantled end-of-life pouch cell: a pouch case (left) anode plate (middle), and cathode plate (right), and (b) the materials generated after the delamination in water: delaminated aluminium foil (left) and cathode active material (right), and (c) schematic diagram showing the regeneration of $LiFePO_4$ from spent $Li_{1-x}FePO_4$ cathode.

hence good stability with spent LFP powder. Further, ICP-MS of the regenerated material shows the desired stoichiometry of $LiFePO_4$ (*i.e.*, Li : Fe : P atomic ratio is 1.00 : 1.00 : 1.02), illustrating the success of the direct re-lithiation process.

Next, the suitability of $FeCl_3$ as an oxidising agent to selectively leach lithium from spent $Li_{0.91}FePO_4$ was investigated by XRD. $FeCl_3$ was selected due to its strong oxidising behaviour towards less noble metals, and since presence of ferric ions will not contaminate the system with an additional cation. Additionally, cyclic voltammetry of aqueous $FeCl_3$ shows reversible $Fe^{II/III}$ redox and hence it is likely redox-recyclable.[33,34] Systematic investigation of the effects of temperature, solid to liquid (S/L) ratio, $FeCl_3$ concentration, and reaction time on the structural conversion and hence lithium removal ($Li_{0.91}FePO_4$ to $FePO_4$) are shown in Fig. S7.† Within the parameter space examined, optimised reaction conditions of 0.75 mol dm^{-3} $FeCl_3$ at 25 °C with a S/L ratio of 150 g L^{-1} yielded full conversion in 0.5 h. These conditions are relatively mild compared to literature processes, where H_2O_2 or concentrated sulfuric acid are commonly used to leach spent LFP.[29,35,36] XRD patterns of

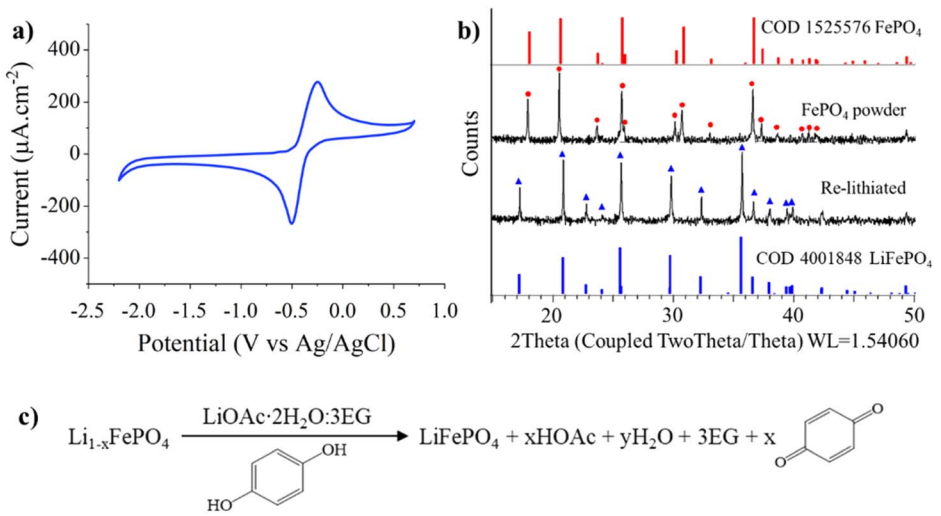

Fig. 2 (a) Cyclic voltammograms of 20 mmol dm^{-3} of hydroquinone in $LiOAc \cdot 2H_2O$:3EG solution. Scans are recorded at 25 °C at a scan rate of 20 mV s^{-1}, using a graphite disk working electrode, and an aqueous 3.0 mol dm^{-3} KCl silver/silver chloride reference electrode, (b) XRD patterns showing the conversion of $FePO_4$ to $LiFePO_4$ with hydroquinone in $LiOAc \cdot 2H_2O$:3EG solution, and (c) chemical reaction for conversion of $Li_{1-x}FePO_4$ to $LiFePO_4$ by hydroquinone in $LiOAc \cdot 2H_2O$:3EG solution.

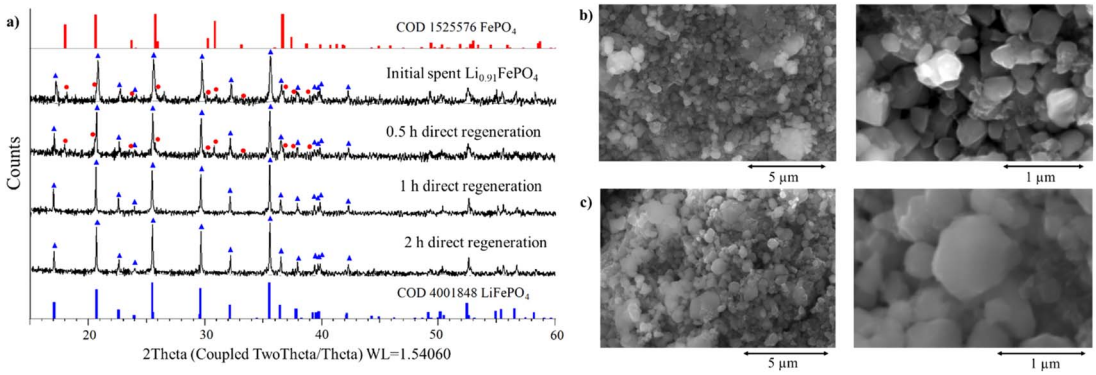

Fig. 3 (a) XRD patterns of spent $Li_{0.91}FePO_4$, and materials produced after 0.5–2 h of treatment with hydroquinone in LiOAc·$2H_2O$:3EG at 25 °C, and (b) SEM images showing the morphology of spent $Li_{0.91}FePO_4$ powder, and (c) $LiFePO_4$ re-lithiated using direct reductive re-lithiation with 0.4 g of hydroquinone per 1 g of spent $Li_{1-x}FePO_4$ in 2.1 g of LiOAc·$2H_2O$:3EG at 25 °C for 1 h.

the materials after oxidative leaching and re-lithiation reveal full oxidation of $Li_{0.91}FePO_4$ to $FePO_4$ in the first step and conversion to $LiFePO_4$ (re-lithiation) after 3 h in the second step (Fig. 4a). Corresponding SEM images of the cathode particles (Fig. 4b and c) illustrate that there are no significant changes to the particle size and shape, consistent with the modest 2.59% volume change between $LiFePO_4$ and $FePO_4$ (291.2 $Å^3$ and 271.5 $Å^3$, respectively).[37,38] Elemental analysis by ICP-MS of the ferric chloride solution after leaching shows the presence of Li (3944 ppm), as expected, but also P (313 ppm). While there was an apparent increase in Fe content in the solution after lithium leaching (6.18% increase), it must be noted that this increase was within the error of the measurement and must be treated cautiously. Moreover, the eutectic solution following re-lithiation contains 346 ppm of P and 1242 ppm of Fe. This indicates non-selective leaching when using $FeCl_3$, potentially due to the acidity of the solution (pH is 1.0 before leaching and 1.4 after leaching), and structural instability across the two-step process.

The electrochemical properties of the direct regenerated $LiFePO_4$ and the spent $Li_{0.91}FePO_4$ active material are discussed in this section, while active material from oxidative leaching/$LiFePO_4$ regeneration method displayed poor electrochemical behaviour, possibly related to the instability noted in the two-step process. The spent $Li_{0.91}FePO_4$ and direct re-lithiated material were treated at 450 °C for 1 h in an argon atmosphere to convert the remaining polymer binder to carbon before making cathodes. Fig. 5a exhibits the cyclic voltammograms of the directly regenerated and spent $Li_{0.91}FePO_4$ at a scan rate of 0.2 mV s^{-1} in the potential range of 2.0–4.5 V (*vs.* Li^+/Li). The oxidation and reduction onset values for the $Fe^{II/III}$ redox couple of direct regenerated and spent $Li_{0.91}FePO_4$ are 3.42 V and 3.46 V, respectively. The curves have pleasing symmetry corresponding to good reversible electrochemical reactions of $Fe^{II/III}$ during the lithiation and de-lithiation processes.

Charge–discharge potential profiles for directly regenerated $LiFePO_4$ at different C-rates are shown in Fig. 5b and c. At 0.1C

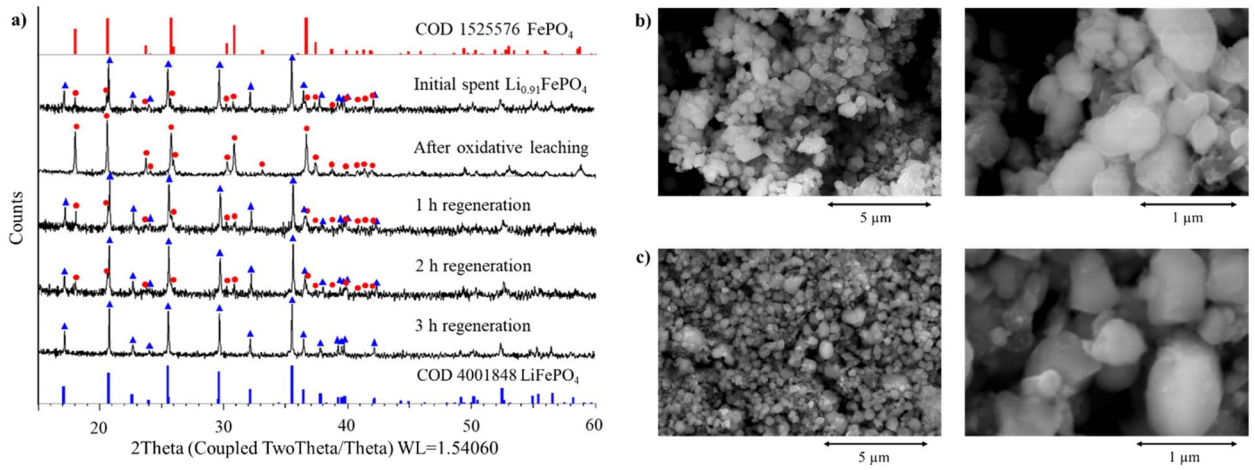

Fig. 4 (a) XRD patterns of initial spent $Li_{0.91}FePO_4$, leaching residue after oxidative leaching with 0.75 mol dm^{-3} $FeCl_3$ in water at 25 °C for 0.5 h (S : L = 150 g L^{-1}), and material regenerated with hydroquinone in LiOAc·$2H_2O$:3EG at 25 °C for 1 h, 2 h, and 3 h, and (b) SEM images of oxidative leached powder (water + 1 mol dm^{-3} $FeCl_3$), and (c) subsequent reductive regenerated $LiFePO_4$ with 0.4 g of hydroquinone per 1 g of spent $Li_{0.91}FePO_4$ in 2.1 g of LiOAc·$2H_2O$:3EG at 25 °C for 3 h.

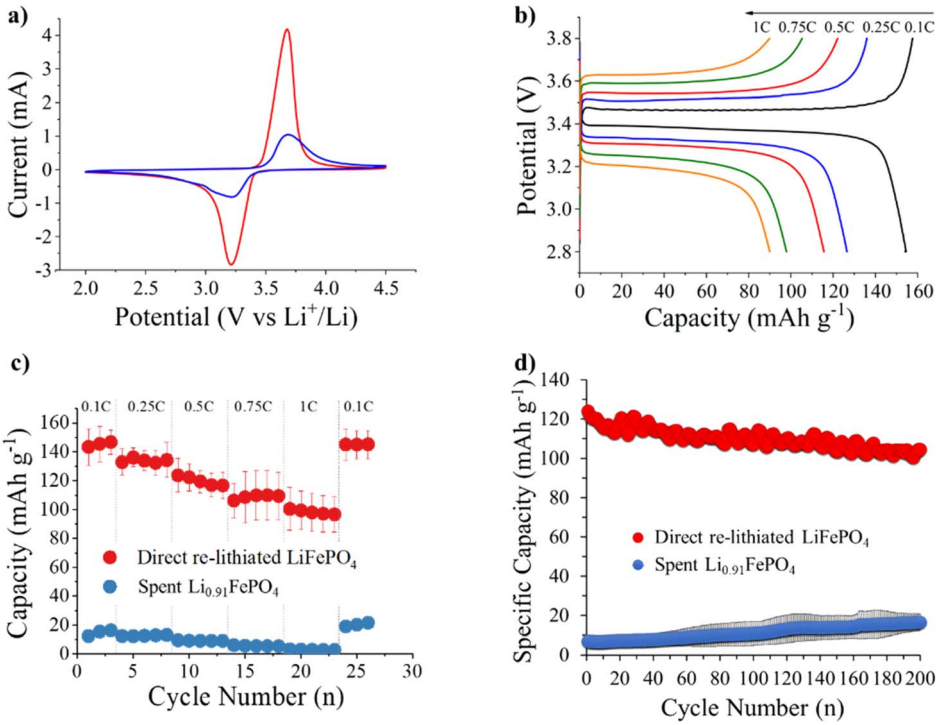

Fig. 5 (a) Cyclic voltammetry curves at a scan rate of 0.2 mV s^{-1} of direct re-lithiated $LiFePO_4$ (b) the first charge and discharge curves of direct re-lithiated $LiFePO_4$ at different discharge rates, (c) and (d) are rate capability, and cycle performance at 0.5C of direct re-lithiated $LiFePO_4$ and spent $Li_{0.91}FePO_4$.

(calculated assuming a practical capacity of 155 mA h g^{-1}) the potential curve shows the characteristic potential plateau at 3.46 V. The discharge capacity drops with the increase of the current density due to sluggish Li^+ kinetics at a higher rate.[39] Specific discharge capacities of 153.9, 126.6, 115.5, 97.9, and 90.0 mA h g^{-1} can be obtained at 0.1C, 0.25C, 0.5C, 0.75C, and 1C, respectively for the directly regenerated $LiFePO_4$ (Fig. 5c). Moreover, the capacity is fully recovered (151.4 mA h g^{-1}) after returning to 0.1C, indicating good electrochemical reversibility.

Fig. 5d shows the cycle performance comparison of the regenerated $LiFePO_4$ and spent $Li_{0.91}FePO_4$ cathode within the potential range of 2.8–3.8 V (*vs.* Li^+/Li) at 0.5C. It can be seen that the discharge capacity of the regenerated cathode material is approx. 120 mA h g^{-1}, with 88% capacity retention after 200 cycles. This clearly demonstrates the effectiveness of the regeneration approach introduced herein, with additional performance enhancement likely through well-established material/electrode optimisation. The capacity of the regenerated $LiFePO_4$ is dramatically improved from the spent material, which exhibits a low capacity of 20 mA h g^{-1} at 0.1C. Since the history of the pouch cell prior to disassembly is not known, it is difficult to comment further on the cause(s) for this. One possibility is that there is a conductive carbothermal coating on the surface of the LFP particles[40] that has been damaged during the oxidative or relithiation steps. Alternatively, the presence of an inert iron phosphorous phase has been proposed.[41] $Fe_2P_2O_7$ coatings have been observed in XRD patterns of LFP as small peaks between 28 and 33° 2Theta.[41] No additional peaks are detected in Fig. 3a or Fig. 4a that could be relating to the formation of these complexes during the oxidation or relithiation processes. Note that the electrochemical properties of LFP rejuvenated *via* direct recycling process will also depend on the initial crystal structure, particle shape and size of the spent materials.

Overall, direct re-lithiation using hydroquinone as a recyclable reducing agent, as demonstrated in this work, provides a more environmentally sustainable closed-loop process and economic advantages for recycling compared to current high-temperature hydrometallurgical approaches. Critically, this re-lithiation process can be carried out at room temperature and under standard atmospheric conditions without special safety considerations.

While the oxidative leaching/$LiFePO_4$ regeneration method did not produce a high-performance material in this study, the approach may nonetheless be important in the future to isolate Li and/or $FePO_4$. For example, selective leaching of Li from battery materials, including LFP, may be a critical process to enable the manufacture of LIBs with 10% recycled Li from 2035, in line with EU regulations.[42] Further, the residual $FePO_4$ can be re-used as a raw material to synthesise LFP by conventional synthetic routes.[43–45]

Conclusions

This study has demonstrated a simple, low-temperature recycling strategy for spent $Li_{1-x}FePO_4$ cathode material. The direct re-lithiation method uses readily available reagents, such as hydroquinone, as the reducing agent in a liquid formed from

$LiOAc{\cdot}2H_2O$:3EG. The electrochemical properties of the regenerated $LiFePO_4$ are significantly improved compared to the original spent $Li_{0.91}FePO_4$ material, indicating the potential to be directly reused in batteries.

A second process based on a literature approach was developed which initially carried out oxidation of the spent cathode material (involving Li leaching), followed by a reductive regeneration. Although this process increased the activity of the regenerated material it was slower, involved more chemicals and resulted in a significantly lower discharge capacity compared to the directly re-lithiated process.

Most studies conclude that the regeneration of LFP cathode material cannot be made economically and carbon negative compared to synthesis of virgin LFP. This is due to the high temperature and complexity of previously described methods. The simplicity of the direct re-lithiation process coupled with the low temperature could result in a carbon negative and inexpensive regeneration although it must be acknowledged that an optimal process requires the lithium loop to be closed using a stable lithium source which can regenerate the hydroquinone and re-lithiate the liquid.

Conflicts of interest

There are no conflicts to declare.

Acknowledgements

The authors would like to thank the Faraday Institution (award number FIRG027, project website: **https://relib.org.uk/**) for funding this work. TY acknowledges support from the Royal Thai Government Scholarship, the Suranaree University of Technology, and Johnson Matthey. WMD acknowledges support from the Faraday Institution [grant number FIRG044]. The authors would also like to thank Johnson Matthey for providing the spent lithium iron phosphate battery and Roberto Sommerville (University of Birmingham) for dismantling the battery used within this work.

Notes and references

1 M.-K. Tran, A. DaCosta, A. Mevawalla, S. Panchal and M. Fowler, *Batteries*, 2021, **7**, 51.
2 T. Feng, W. Guo, Q. Li, Z. Meng and W. Liang, *J. Energy Storage*, 2022, **52**, 104767.
3 R. Sommerville, P. Zhu, M. A. Rajaeifar, O. Heidrich, V. Goodship and E. Kendrick, *Resour. Conserv. Recycl.*, 2021, **165**, 105219.
4 G. Harper, R. Sommerville, E. Kendrick, L. Driscoll, P. Slater, R. Stolkin, A. Walton, P. Christensen, O. Heidrich, S. Lambert, A. Abbott, K. Ryder, L. Gaines and P. Anderson, *Nature*, 2019, **575**, 75–86.
5 B. Jones, R. J. R. Elliott and V. Nguyen-Tien, *Appl. Energy*, 2020, **280**, 115072.
6 Y. Wang, N. An, L. Wen, L. Wang, X. Jiang, F. Hou, Y. Yin and J. Liang, *J. Energy Chem.*, 2021, **55**, 391–419.
7 Q. Yan, A. Ding, M. Li, C. Liu and C. Xiao, *Energy Fuels*, 2023, **37**, 1216–1224.
8 C. Yang, J.-l. Zhang, Q.-k. Jing, Y.-b. Liu, Y.-q. Chen and C.-y. Wang, *Int. J. Miner. Metall. Mater.*, 2021, **28**, 1478–1487.
9 P. Yadav, C. J. Jie, S. Tan and M. Srinivasan, *J. Hazard. Mater.*, 2020, **399**, 123068.
10 K. Liu, S. Yang, F. Lai, Q. Li, H. Wang, T. Tao, D. Xiang and X. Zhang, *Ionics*, 2021, **27**, 5127–5135.
11 J. Kumar, X. Shen, B. Li, H. Liu and J. Zhao, *Waste Manage.*, 2020, **113**, 32–40.
12 P. Liu, J. Wang, J. Hicks-Garner, E. Sherman, S. Soukiazian, M. W. Verbrugge, H. Tataria, J. W. Musser and P. Finamore, *J. Electrochem. Soc.*, 2010, **157**, A499.
13 C. Wu, J. Hu, L. Ye, Z. Su, X. Fang, X. Zhu, L. Zhuang, X. Ai, H. Yang and J. Qian, *ACS Sustain. Chem. Eng.*, 2021, **9**, 16384–16393.
14 Y. Gao, Y. Li, J. Li, H. Xie and Y. Chen, *J. Alloys Compd.*, 2020, **845**, 156234.
15 J. Li and Z.-F. Ma, *Chem*, 2019, **5**, 3–6.
16 J. Wang, Q. Zhang, J. Sheng, Z. Liang, J. Ma, Y. Chen, G. Zhou and H.-M. Cheng, *Natl. Sci. Rev.*, 2022, **9**, nwac097.
17 X. Liu, M. Wang, L. Deng, Y.-J. Cheng, J. Gao and Y. Xia, *Ind. Eng. Chem. Res.*, 2022, **61**, 3831–3839.
18 A. P. Abbott, G. Frisch, J. Hartley and K. S. Ryder, *Green Chem.*, 2011, **13**, 471–481.
19 B. Tang, H. Zhang and K. H. Row, *J. Sep. Sci.*, 2015, **38**, 1053–1064.
20 E. L. Smith, A. P. Abbott and K. S. Ryder, *Chem. Rev.*, 2014, **114**, 11060–11082.
21 A. P. Abbott, *Curr. Opin. Green Sustainable Chem.*, 2022, **36**, 100649.
22 S. Wang, Z. Zhang, Z. Lu and Z. Xu, *Green Chem.*, 2020, **22**, 4473–4482.
23 D. L. Thompson, I. M. Pateli, C. Lei, A. Jarvis, A. P. Abbott and J. M. Hartley, *Green Chem.*, 2022, **24**, 4877–4886.
24 G. Zante, A. Braun, A. Masmoudi, R. Barillon, D. Trébouet and M. Boltoeva, *Miner. Eng.*, 2020, **156**, 106512.
25 P. G. Schiavi, P. Altimari, M. Branchi, R. Zanoni, G. Simonetti, M. A. Navarra and F. Pagnanelli, *Chem. Eng. J.*, 2021, **417**, 129249.
26 N. Peeters, K. Binnemans and S. Riaño, *Green Chem.*, 2020, **22**, 4210–4221.
27 V. N. H. Nguyen and M. S. Lee, *Physicochem. Probl. Miner. Process.*, 2020, **56**, 599–610.
28 N. Vieceli, N. Reinhardt, C. Ekberg and M. Petranikova, *Metals*, 2021, **11**, 54.
29 Y. Niu, X. Peng, J. Li, Y. Zhang, F. Song, D. Shi and L. Li, *Chin. J. Chem. Eng.*, 2023, **54**, 306–315.
30 D. Thompson, C. Hyde, J. M. Hartley, A. P. Abbott, P. A. Anderson and G. D. J. Harper, *Resour. Conserv. Recycl.*, 2021, **175**, 105741.
31 S. Scott, J. Terreblanche, D. L. Thompson, C. Lei, J. M. Hartley, A. P. Abbott and K. S. Ryder, *J. Phys. Chem. C*, 2022, **126**, 8489–8498.
32 K. Park, J. Yu, J. Coyle, Q. Dai, S. Frisco, M. Zhou and A. Burrell, *ACS Sustain. Chem. Eng.*, 2021, **9**, 8214–8221.

33 J. Xu, Q. Ma, H. Su, F. Qiao, P. Leung, A. Shah and Q. Xu, *Ionics*, 2020, **26**, 483–492.
34 K. L. Hawthorne, J. S. Wainright and R. F. Savinell, *J. Electrochem. Soc.*, 2014, **161**, A1662.
35 W.-b. Lou, Y. Zhang, Y. Zhang, S.-l. Zheng, P. Sun, X.-j. Wang, J.-z. Li, S. Qiao, Y. Zhang, M. Wenzel and J. J. Weigand, *Trans. Nonferrous Metals Soc. China*, 2021, **31**, 817–831.
36 F. Larouche, F. Tedjar, K. Amouzegar, G. Houlachi, P. Bouchard, G. P. Demopoulos and K. Zaghib, *Materials*, 2020, **13**, 801.
37 W.-J. Zhang, *J. Power Sources*, 2011, **196**, 2962–2970.
38 F. Schipper and D. Aurbach, *Russ. J. Electrochem.*, 2016, **52**, 1095–1121.
39 Y. Song, B. Xie, S. Song, S. Lei, W. Sun, R. Xu and Y. Yang, *Green Chem.*, 2021, **23**, 3963–3971.
40 Z. Chen and J. R. Dahn, *J. Electrochem. Soc.*, 2002, **149**, A1184.
41 Y. Liu, J. Wang, J. Liu, M. N. Banis, B. Xiao, A. Lushington, W. Xiao, R. Li, T.-K. Sham, G. Liang and X. Sun, *Nano Energy*, 2018, **45**, 52–60.
42 European Commission, *Concerning batteries and waste batteries, repealing directive 2006/66/EC and amending regulation (EU) No 2019/1020*, 2020, **https://eur-lex.europa.eu/legal-content/EN/TXT/?uri=celex%3A52020PC0798**.
43 B. Chen, M. Liu, S. Cao, G. Chen, X. Guo and X. Wang, *Mater. Chem. Phys.*, 2022, **279**, 125750.
44 D. Peng, J. Zhang, J. Zou, G. Ji, L. Ye, D. Li, B. Zhang and X. Ou, *J. Clean. Prod.*, 2021, **316**, 128098.
45 H. Jin, J. Zhang, D. Wang, Q. Jing, Y. Chen and C. Wang, *Green Chem.*, 2022, **24**, 152–162.